Statistically Accurate Low Order Models for Uncertainty Quantification in Turbulent Dynamical Systems - Supplementary material

Themistoklis P. Sapsis and Andrew J. Majda
Courant Institute of Mathematical Sciences, New York University,
251 Mercer St., New York, 10012 NY

July 9, 2013

1 Forty mode L-96 system

Here we present additional results of the ROMQG algorithm for the L-96 system using deterministic periodic or stochastic forcing. We are studying the case of $F = 6$ (weakly chaotic), $F = 8$ (strongly chaotic), and $F = 16$ (turbulent) regime. A typical synaptic of the field for each case is presented in Figure S1.

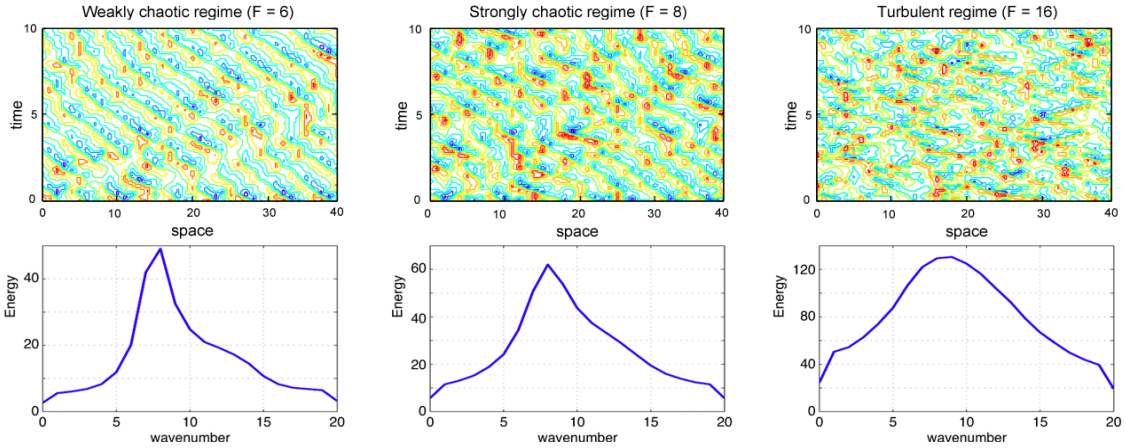

Figure S1: Numerical solutions and corresponding spectra of L-96 model in space-time for weakly chaotic ($F = 6$), strongly chaotic ($F = 8$), and fully turbulent ($F = 16$) regime.

In Figures S2-S4 we present the ROMQG response for a random forcing fluctuating around $F = 6$ (Fig. S2), as well as for a periodic and random forcing in the turbulent regime, $F = 16$ (Fig. S3-S4). Various orders of truncation are considered ranging from 1 to 4 Fourier modes. The results are presented in terms of the Fourier modes energy as well as the energy of the mean and they are compared with direct Monte-Carlo simulations.

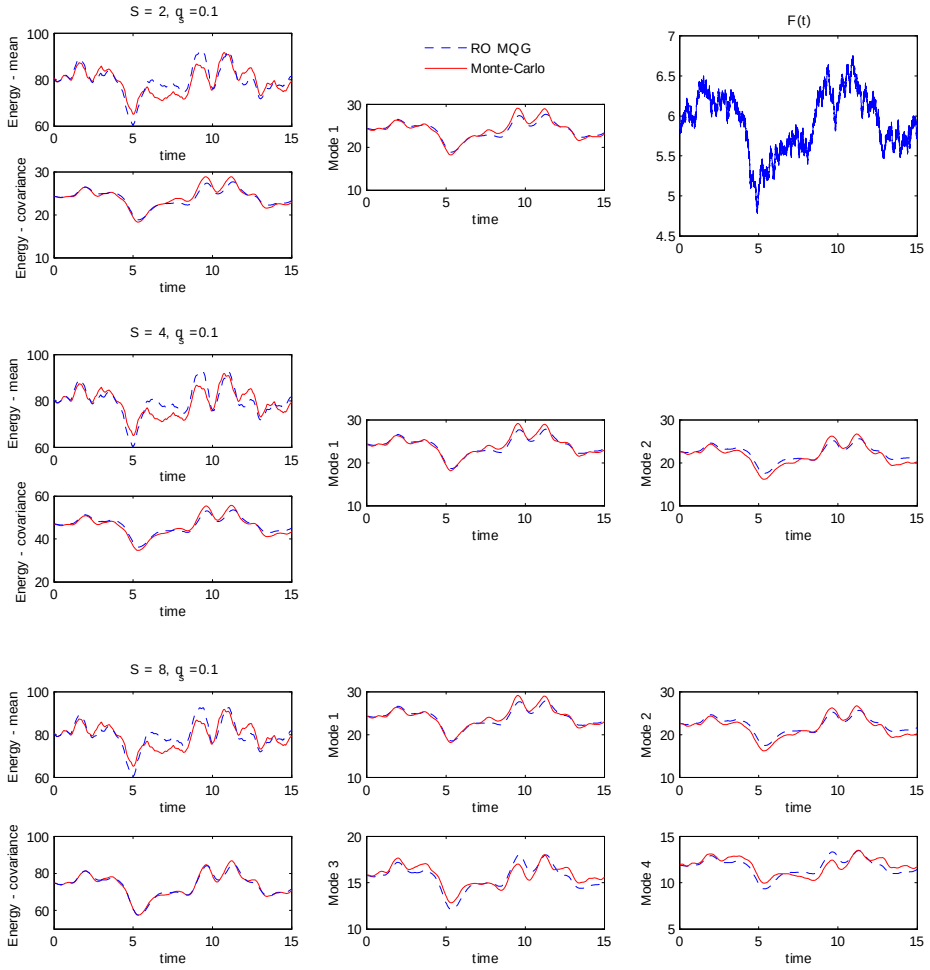

Figure S2: Comparison of ROMQG with Monte-Carlo for random forcing fluctuating aroung $F = 6$. Results are presented using 1 leading wavenumber (S =2 real modes), 2 leading wavenumbers ($S = 4$ real modes), and 4 leading wavenumbers ($S = 8$ real modes).

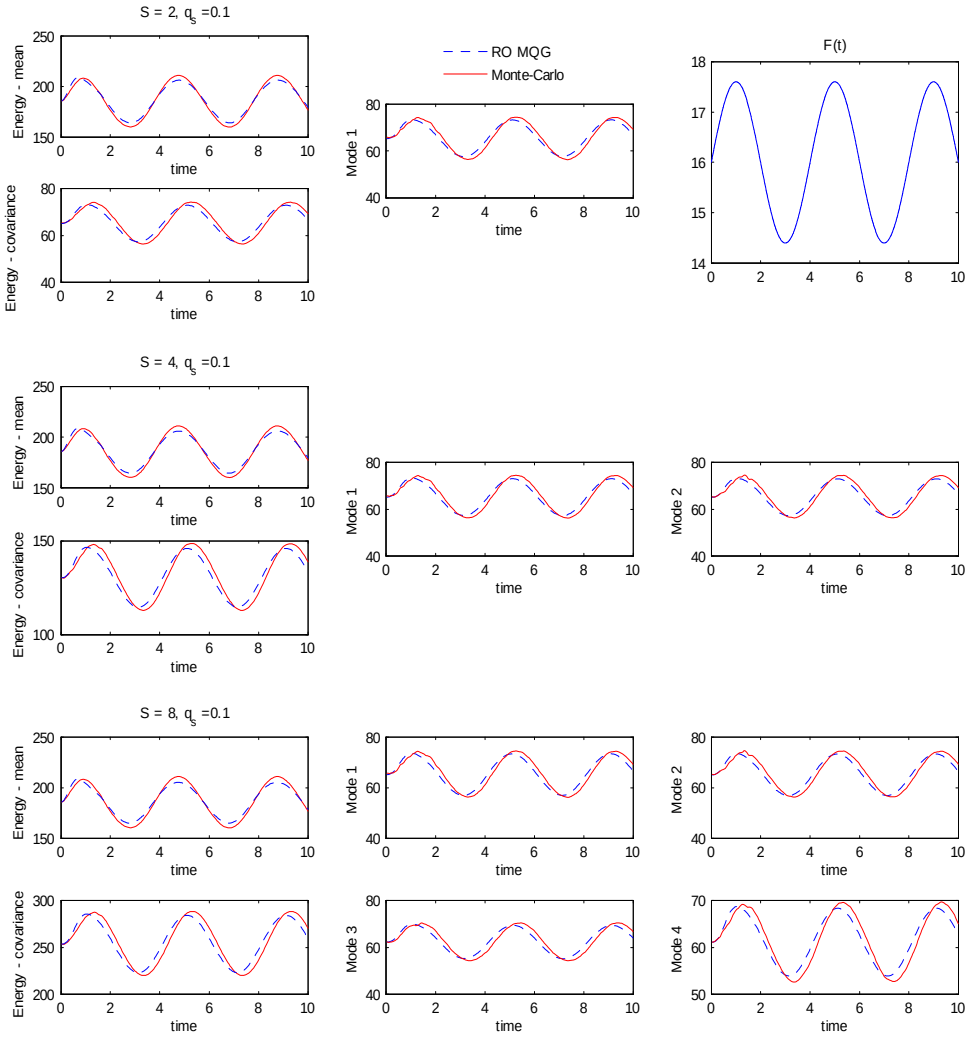

Figure S3: Comparison of ROMQG with Monte-Carlo for periodic forcing fluctuating aroung $F = 16$. Results are presented using 1 leading wavenumber (S =2 real modes), 2 leading wavenumbers ($S = 4$ real modes), and 4 leading wavenumbers ($S = 8$ real modes).

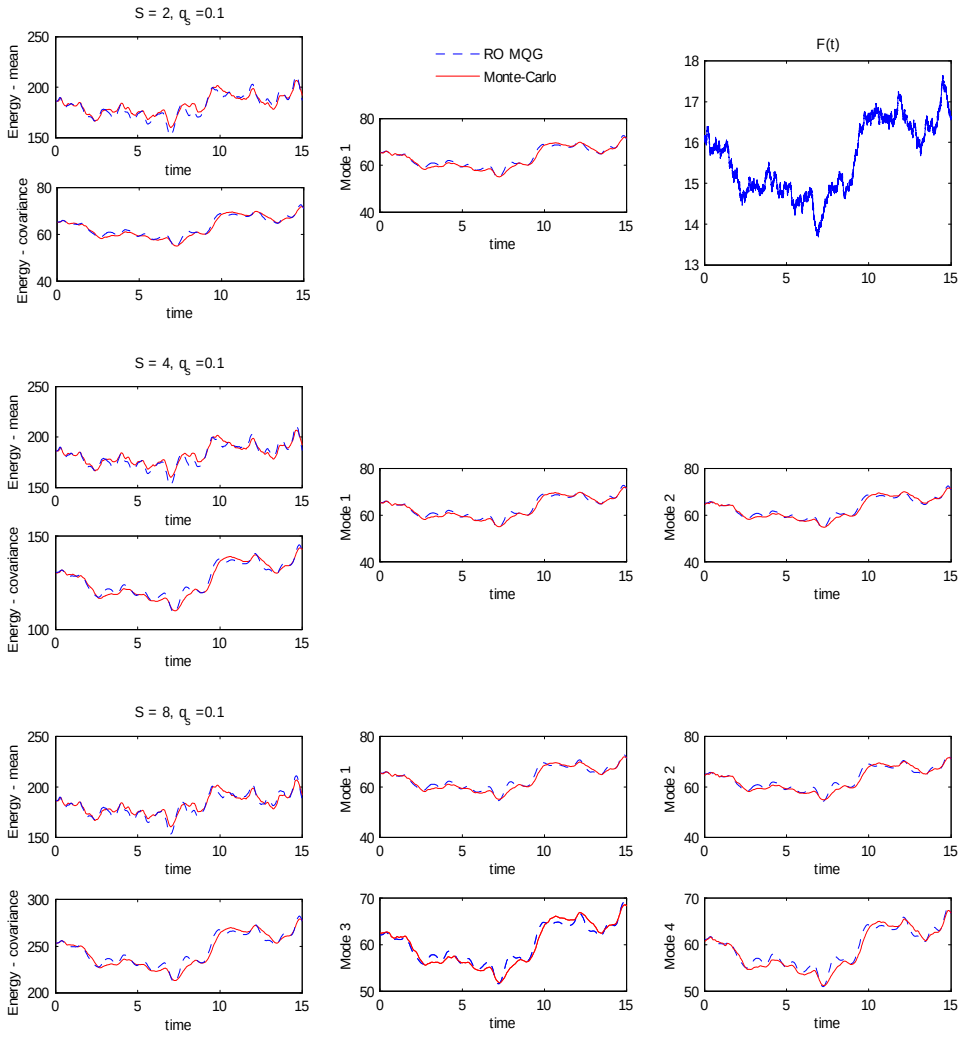

Figure S4: Comparison of ROMQG with Monte-Carlo for random forcing fluctuating aroung $F = 16$. Results are presented using 1 leading wavenumber (S =2 real modes), 2 leading wavenumbers ($S = 4$ real modes), and 4 leading wavenumbers ($S = 8$ real modes).

2 Two-layer baroclinic model

We consider the Phillips model in a barotropic-baroclinic mode formulation with periodic boundary conditions given by

$$\frac{\partial q_\psi}{\partial t} + J\left(\psi, q_\psi\right) + J\left(\tau, q_\tau\right) + \beta\frac{\partial \psi}{\partial x} + U\frac{\partial}{\partial x}\nabla^2\tau = -\left(1-\delta\right)r\nabla^2\left(\psi - a^{-1}\tau\right)$$

$$\frac{\partial q_\tau}{\partial t} + J\left(\psi, q_\tau\right) + J\left(\tau, q_\psi\right) + \xi J\left(\tau, q_\tau\right) + \beta\frac{\partial \tau}{\partial x} + U\frac{\partial}{\partial x}\left(\nabla^2\psi + \lambda^2\psi + \xi\nabla^2\tau\right) = \sqrt{\delta\left(1-\delta\right)}r\nabla^2\left(\psi - a^{-1}\tau\right)$$

where $q_\psi = \nabla^2\psi$ and $q_\tau = \nabla^2\tau - \lambda^2\tau$. For what follows we will use the quadratic operator associated with the above system

$$\mathbf{B}\left(\mathbf{q}_1, \mathbf{q}_2\right) = -\begin{pmatrix} J\left(\psi_1, q_{2,\psi}\right) + J\left(\tau_1, q_{2,\tau}\right) \\ J\left(\psi_1, q_{2,\tau}\right) + J\left(\tau_1, q_{2,\psi}\right) + \xi J\left(\tau_1, q_{2,\tau}\right) \end{pmatrix}$$

as well as the linear operator

$$\mathbf{L}\left(\mathbf{q}\right) = \begin{pmatrix} -\left(1-\delta\right)r\nabla^2\left(\psi - a^{-1}\tau\right) - U\frac{\partial}{\partial x}\nabla^2\tau - \beta\frac{\partial \psi}{\partial x} \\ \sqrt{\delta\left(1-\delta\right)}r\nabla^2\left(\psi - a^{-1}\tau\right) - \beta\frac{\partial \tau}{\partial x} - U\frac{\partial}{\partial x}\left(\nabla^2\psi + \lambda^2\psi + \xi\nabla^2\tau\right) \end{pmatrix}.$$

Using the above notation the original system can be written as

$$\frac{d\mathbf{q}}{dt} = \mathbf{L}\left(\mathbf{q}\right) + \mathbf{B}\left(\mathbf{q}, \mathbf{q}\right).$$

The parameters values are given in the paper and they correspond to baroclinic ocean turbulence at high latitudes. A typical snapshot of the vorticity fields q_ψ, q_τ is given in Figure S5.

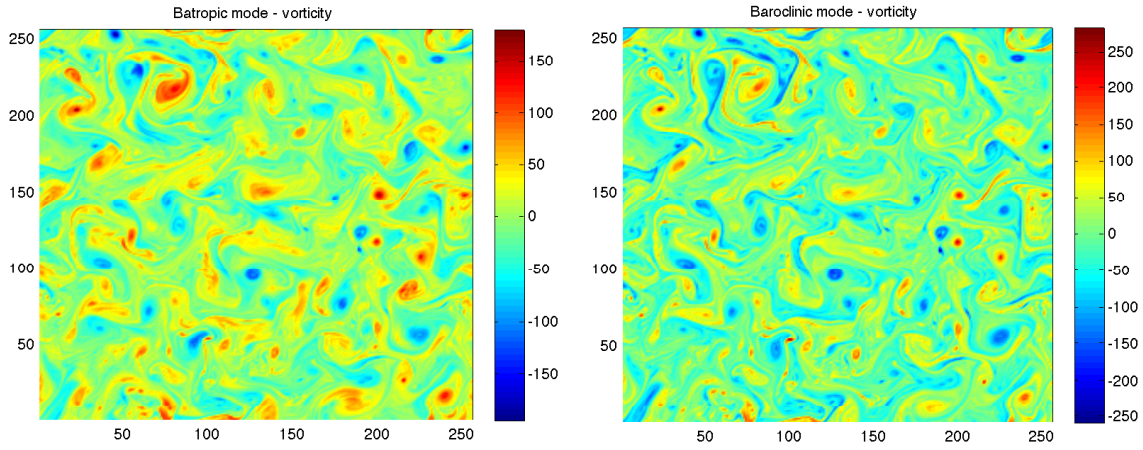

Figure S5: Typical snapshots (vorticity fields) of the barotropic and baroclinic mode for baroclinic ocean turbulence at high latitudes.

2.1 Setup and basic properties

The inner product that corresponds to the total energy is given by the following bilinear form

$$\begin{aligned}[\mathbf{q}_1, \mathbf{q}_2]_E &= \int \nabla\psi_1 \nabla\psi_2^* + \nabla\tau_1 \nabla\tau_2^* + \lambda^2 \tau_1 \tau_2^* \\ &= -\int q_{\psi 1}\psi_2^* + q_{\tau 1}\tau_2^* \\ &= \int \left(k^2 + l^2\right)\left(\hat{\psi}_1 \hat{\psi}_2^*\right) + \left(k^2 + l^2 + \lambda^2\right)\left(\hat{\tau}_1 \hat{\tau}_2^*\right)\end{aligned}$$

where the hats denote the spatial Fourier transforms.

We will now prove that the quadratic operator is conservative with respect to this inner product. In particular we have (using the second expression for the energy inner product)

$$\left[\mathbf{B}\left(\mathbf{q},\mathbf{q}\right),\mathbf{q}\right]_E = \int \left(J\left(\psi, q_\psi\right)\psi + J\left(\tau, q_\tau\right)\psi + J\left(\psi, q_\tau\right)\tau + J\left(\tau, q_\psi\right)\tau + \xi J\left(\tau, q_\tau\right)\tau\right)$$

and

$$\int J\left(\psi, q_\psi\right)\psi = \int \psi \nabla^\perp \psi . \nabla q_\psi = \frac{1}{2}\int \nabla^\perp \psi^2 . \nabla q_\psi = \frac{1}{2}\int q_\psi \operatorname{div} \nabla^\perp \psi^2 = 0,$$

where we used Greens identity and took into account the periodic boundary conditions. Similarly we can obtain $\int J\left(\tau, q_\tau\right)\tau = \int J\left(\tau, q_\psi\right)\tau = 0$.

In addition,

$$\int J\left(\tau, q_\tau\right)\psi + J\left(\psi, q_\tau\right)\tau = \int \psi \nabla^\perp \tau . \nabla q_\tau + \tau \nabla^\perp \psi . \nabla q_\tau = \int \nabla^\perp\left(\psi\tau\right) . \nabla q_\tau = \int q_\tau \operatorname{div} \nabla^\perp\left(\psi\tau\right) = 0$$

with the orthogonal gradient of τ given by $\nabla^\perp \tau = \left(-\frac{\partial \tau}{\partial y}, \frac{\partial \tau}{\partial x}\right)^T$. Therefore, the quadratic terms conserve energy

$$\left[\mathbf{B}\left(\mathbf{q},\mathbf{q}\right),\mathbf{q}\right]_E = 0.$$

2.2 Mean field dynamics

We obtain the equation for the mean vorticity by expanding the solution in terms of Fourier modes which is the natural basis since the problem is defined on a periodic domain. In particular we represent the solution as

$$\mathbf{q}\left(t, \mathbf{x}; \omega\right) = \bar{\mathbf{q}}\left(t, \mathbf{x}\right) + \sum_{k,l} \mathbf{q}_{kl}\left(t, \mathbf{x}; \omega\right)$$

where $\mathbf{q}_{kl}\left(t, \mathbf{x}; \omega\right)$ have the form $\mathbf{q}_{kl}\left(t, \mathbf{x}; \omega\right) = \hat{\mathbf{q}}_{kl} e^{i(kx+ly)}$and for the steady state we have

$$\frac{d\bar{\mathbf{q}}_\infty}{dt} = 0 = \mathbf{L}\left(\bar{\mathbf{q}}_\infty\right) + \mathbf{B}\left(\bar{\mathbf{q}}_\infty, \bar{\mathbf{q}}_\infty\right) + \sum_{k,l,m,n} \overline{\frac{\mathbf{B}\left(\mathbf{q}_{kl}, \mathbf{q}_{mn}\right) + \mathbf{B}^*\left(\mathbf{q}_{kl}, \mathbf{q}_{mn}\right)}{2}}$$

Note that because different wavenumbers will be uncorrelated in steady state, we will have

$$\sum_{k,l,m,n} \overline{\frac{\mathbf{B}\left(\mathbf{q}_{kl}, \mathbf{q}_{mn}\right) + \mathbf{B}^*\left(\mathbf{q}_{kl}, \mathbf{q}_{mn}\right)}{2}} = \sum_{k,l} \overline{\frac{\mathbf{B}\left(\mathbf{q}_{kl}, \mathbf{q}_{kl}\right) + \mathbf{B}^*\left(\mathbf{q}_{kl}, \mathbf{q}_{kl}\right)}{2}}$$

Moreover, we can easily observe that $\mathbf{B}(\mathbf{q}_{kl}, \mathbf{q}_{kl}) = 0$, therefore the equation for the mean decouples from the second order statistics and we obtain:

$$\mathbf{L}(\bar{\mathbf{q}}_\infty) + \mathbf{B}(\bar{\mathbf{q}}_\infty, \bar{\mathbf{q}}_\infty) = 0$$

From which we have

$$\bar{\mathbf{q}}_\infty = 0$$

Thus the mean will not be included in the analysis that follows.

2.3 Dynamics in spectral space

The solution can be represented as

$$\mathbf{q} = \sum_{k,l} \begin{pmatrix} \hat{q}_{kl,\psi} \\ \hat{q}_{kl,\tau} \end{pmatrix} e^{i(kx+ly)}$$

From the above representation we easily obtain an expression for the corresponding streamfunctions

$$q_\psi = \nabla^2 \psi \Rightarrow \psi = -\sum_{k,l} \frac{\hat{q}_{kl,\psi}}{k^2+l^2} e^{i(kx+ly)}$$

$$q_\tau = \nabla^2 \tau - \lambda^2 \tau \Rightarrow \tau = -\sum_{k,l} \frac{\hat{q}_{kl,\tau}}{k^2+l^2+\lambda^2} e^{i(kx+ly)}$$

We saw that the quadratic operator conserves energy and therefore the energy inner product is suitable for formulating an MQG UQ scheme. We use the following spectral variables for which the energy inner product is expressed as Euclidian inner product

$$\hat{p}_{kl,\psi} \equiv \sqrt{k^2+l^2}\hat{\psi}_{kl} = -\frac{\hat{q}_{kl,\psi}}{\sqrt{k^2+l^2}},$$

$$\hat{p}_{kl,\tau} \equiv \sqrt{k^2+l^2+\lambda^2}\hat{\tau}_{kl} = -\frac{\hat{q}_{kl,\tau}}{\sqrt{k^2+l^2+\lambda^2}}$$

With this choice we have

$$[\mathbf{q}_1, \mathbf{q}_2]_E = \int (\hat{p}_{kl,\psi_1}\hat{p}_{kl,\psi_2} + \hat{p}_{kl,\tau_1}\hat{p}_{kl,\tau_2})$$

and the original system will take the form

$$\frac{d\hat{p}_{kl,\psi}}{dt} = \hat{L}_{p_\psi p_\psi}\hat{p}_{kl,\psi} + \hat{L}_{p_\psi p_\tau}\hat{p}_{kl,\tau} - \frac{1}{\sqrt{k^2+l^2}}\mathbf{B}(\mathbf{q},\mathbf{q}).\tilde{\mathbf{q}}_{kl,\psi}$$

$$\frac{d\hat{p}_{kl,\tau}}{dt} = \hat{L}_{p_\tau p_\psi}\hat{p}_{kl,\psi} + \hat{L}_{p_\tau p_\tau}\hat{p}_{kl,\tau} - \frac{1}{\sqrt{k^2+l^2+\lambda^2}}\mathbf{B}(\mathbf{q},\mathbf{q}).\tilde{\mathbf{q}}_{kl,\tau}$$

where,

$$\hat{L}_{p_\psi p_\psi} = \left[-(1-\delta)\, r + \frac{ik\beta}{k^2+l^2} \right]$$
$$\hat{L}_{p_\psi p_\tau} = (1-\delta)\, r a^{-1} \sqrt{\frac{k^2+l^2}{k^2+l^2+\lambda^2}} - iUk \sqrt{\frac{k^2+l^2}{k^2+l^2+\lambda^2}}$$
$$\hat{L}_{p_\tau p_\psi} = \sqrt{\frac{k^2+l^2}{k^2+l^2+\lambda^2}} \left[\sqrt{\delta\,(1-\delta)} r - ikU \left(1 - \frac{\lambda^2}{k^2+l^2} \right) \right]$$
$$\hat{L}_{p_\tau p_\tau} = -\frac{1}{k^2+l^2+\lambda^2} \left[\sqrt{\delta\,(1-\delta)} r a^{-1} \left(k^2+l^2 \right) - ik\beta + ikU\xi \left(k^2+l^2 \right) \right]$$

and the barotropic and baroclinic nonlinear energy fluxes are given by the terms $-\frac{1}{\sqrt{k^2+l^2}} \mathbf{B}\left(\mathbf{q},\mathbf{q}\right).\tilde{\mathbf{q}}_{kl,\psi}$ and $-\frac{1}{\sqrt{k^2+l^2+\lambda^2}} \mathbf{B}\left(\mathbf{q},\mathbf{q}\right).\tilde{\mathbf{q}}_{kl,\tau}$ respectively.

2.4 MQG formulation

We observe that coupling between different wavenumber is introduced only through the conservative, quadratic operator. In particular the covariance for each wavenumber

$$R_{p,kl} = \begin{pmatrix} \overline{|\hat{p}_{kl,\psi}|^2} & \overline{\hat{p}^*_{kl,\psi} \hat{p}_{kl,\tau}} \\ \overline{\hat{p}^*_{kl,\psi} \hat{p}_{kl,\tau}} & \overline{|\hat{p}_{kl,\tau}|^2} \end{pmatrix}$$

will be governed by the equation

$$\frac{dR_{p,kl}}{dt} = \hat{L}_{p,kl} R_{p,kl} + R_{p,kl} \hat{L}^*_{p,kl} + Q_{p,kl}$$

where

$$\hat{L}_{p,kl} = \begin{pmatrix} \hat{L}_{p_\psi p_\psi}(k,l) & \hat{L}_{p_\psi p_\tau}(k,l) \\ \hat{L}_{p_\tau p_\psi}(k,l) & \hat{L}_{p_\tau p_\tau}(k,l) \end{pmatrix}$$

and $Q_{p,kl}$ expresses the nonlinear energy fluxes due to the quadratic operator - this is modeled through the ROMQG approach. Note that the total energy of the system (kinetic and available potential) is given by $tr\left(R_{p,kl}\right)$.

2.5 Eddy heat flux

The eddy heat flux is proportional to the quantity

$$H_f = \frac{\lambda}{U^2} \overline{\psi_x \tau}.$$

Based on the employed formulation (enstrophy or energy) we will have the following expressions for the eddy heat flux:

$$\begin{aligned} H_f &= \frac{\lambda}{U^2}\overline{\psi_x \tau} \\ &= \frac{\lambda}{U^2}\sum_{k,l}\sum_{r,s} ik\hat{\psi}_{kl}\hat{\tau}_{rs}e^{i([k+r]x+[l+s]y)} \\ &= \frac{\lambda}{U^2}\sum_{k,l}\sum_{r,s} i\frac{k}{\sqrt{k^2+l^2}}\frac{1}{\sqrt{r^2+s^2+\lambda^2}}\hat{p}_{kl,\psi}\hat{p}_{rs,\tau}e^{i([k+r]x+[l+s]y)} \\ &= -\frac{\lambda}{U^2}\sum_{k,l}\sum_{r,s} i\frac{k}{(k^2+l^2)}\frac{1}{(r^2+s^2+\lambda^2)}\hat{q}_{kl,\psi}\hat{q}_{rs,\tau}e^{i([k+r]x+[l+s]y)} \end{aligned}$$

The spatially averaged heat flux will be given by

$$\begin{aligned} \langle H_f \rangle &= \frac{\lambda}{U^2}\sum_{k,l} i\frac{k}{\sqrt{k^2+l^2}}\frac{1}{\sqrt{k^2+l^2+\lambda^2}}\hat{p}_{kl,\psi}\hat{p}^*_{kl,\tau} \\ &= \frac{\lambda}{U^2}\sum_{k,l} i\frac{k}{(k^2+l^2)}\frac{1}{(k^2+l^2+\lambda^2)}\hat{q}_{kl,\psi}\hat{q}^*_{kl,\tau} \end{aligned}$$

2.6 Stability and energy fluxes properties for the two-layer baroclinic model

Here we provide an overview of the stability and energy fluxes properties for the two-layer baroclinic model under the parameters given in the paper. More specifically, in Figure S6 we present the total, baroclinic, and barotropic 1D energy spectra of the solution over different wavenumbers. We also present the 1D heat flux spectrum over different wavenumbers (defined in the previous section) normalized by its maximum intensity. Finally, in the same figure we show the 1D stability indicator that is the maximum growth rate for each wavenumber modulus but also the 1D nonlinear barotropic and baroclinic energy fluxes spectra as those are defined at the end of Section 2.3 of this supplementary material. In Figure S7 we present the growth rate variation for the different perturbation levels of the shear U.

Figures S8 and S9 show the 2D spectra of the corresponding quantities illustrating the strongly two-dimensional character of the system. Figure S8 also shows the non-normal characteristics of the linear operator - a feature that usually leads to important challenges for reduction algorithms.

Figure S10 shows the third-order central moments for the Fourier coefficients when we arrange those with respect to their energy (e.g. indices 1 and 2 describe the barotropic and baroclinic coefficients of the most energetic wavenumber, indices 3 and 4 the second most energetic wavenumber, etc.). In particular, we present a 3D contour that contains third order moments with magnitude larger than 10% of the maximum magnitude of any third order moment. In other words Figure S10 shows the most important triad interactions between EOF modes, i.e. Fourier modes which are arranged with respect to energy. We emphasize that these are shown only for illustration purposes and they are never actually used in the ROMQG algorithm.

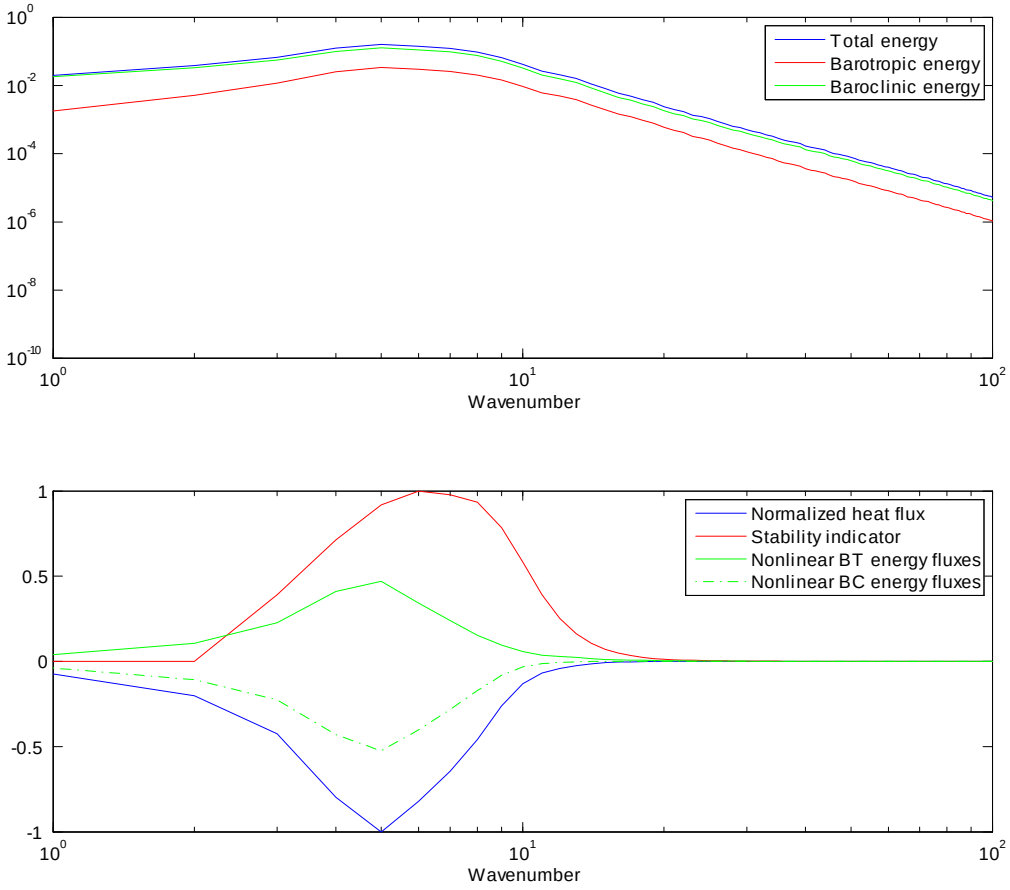

Figure S6: 1D properties for high latitude. Upper plot: Barotropic, baroclinic and total energy with respect to the wavenumber $|\mathbf{k}|$. Lower plot: Wavenumber-averaged heat flux normalized over its maximum value; Stability indicator: $\max_{|\mathbf{k}|=k} \mathrm{Re}\,\lambda_i(\mathbf{k})$ normalized over its maximum magnitude, where $\lambda_i(\mathbf{k})$ are the vertical eigenvalues for each wavenumber; Wavenumber-averaged BT/BC nonlinear energy fluxes.

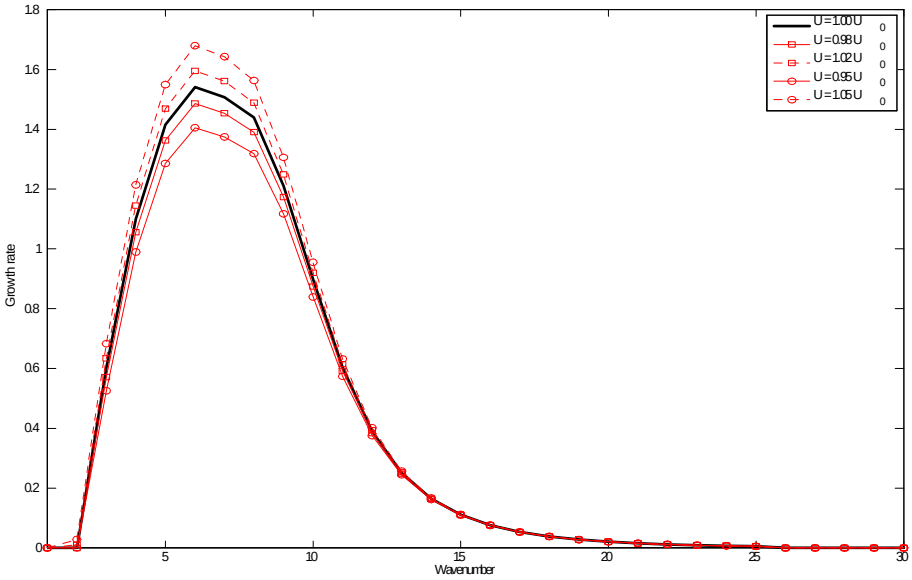

Figure S7: Growth rates of different wavenumbers - computed using the spectral code output.

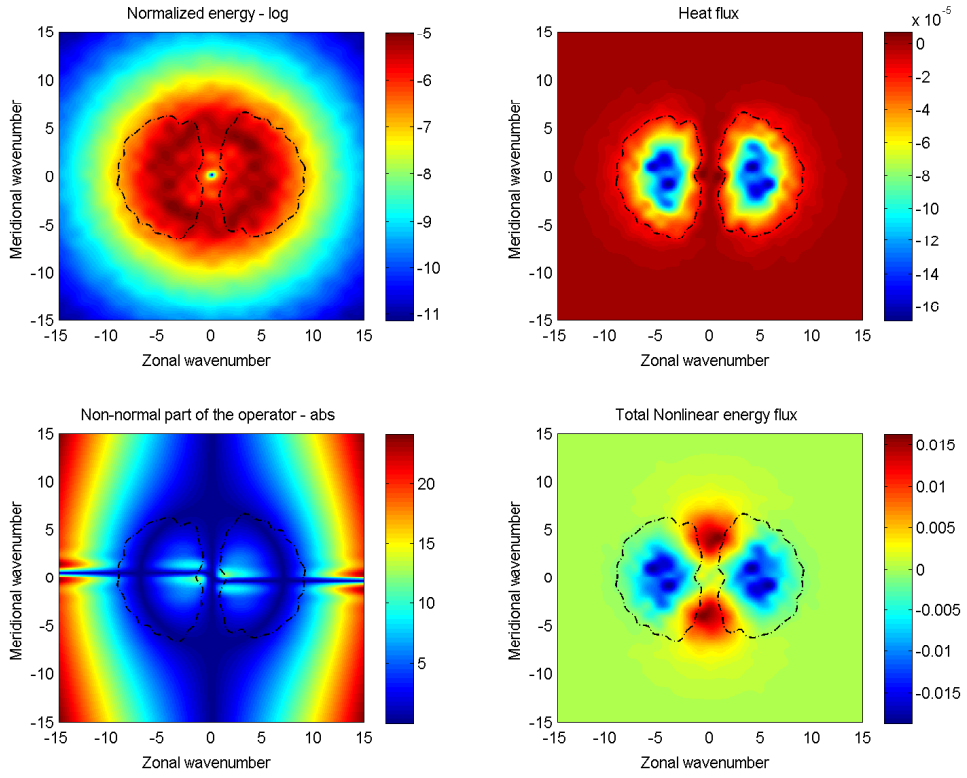

Figure S8: Energy spectrum; Heat flux; magnitude of the non-normal part of the operator: $\left|\hat{L}_{p_\psi p_\tau} - \hat{L}^*_{p_\tau p_\psi}\right|$; Total nonlinear energy flux: $Q_{\tau\tau,kl} + Q_{\psi\psi,kl}$. The black dashed line is the $-10\% \max_{\mathbf{k}} \left|\langle H_f \rangle_{kl}\right|$ contour of the heat flux field.

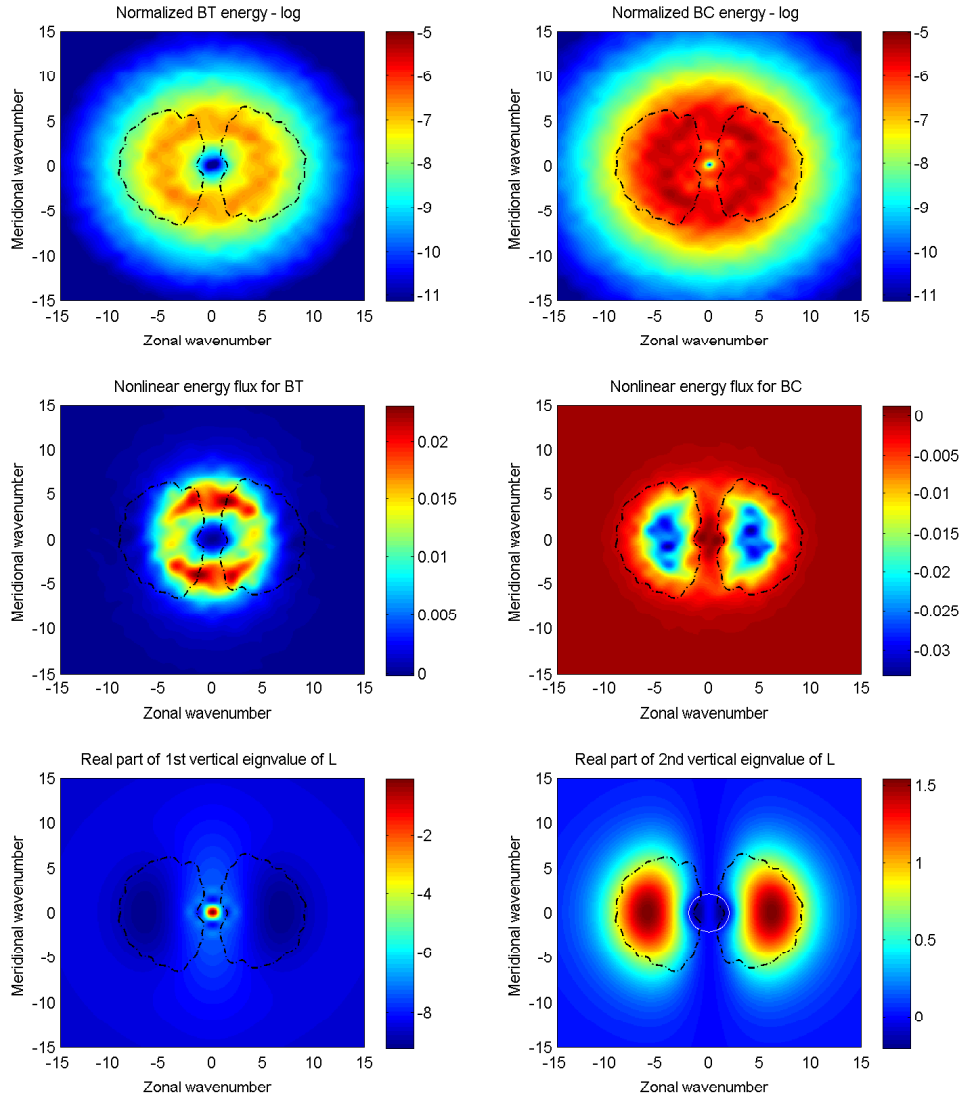

Figure S9: BT and BC energy spectrum; BT and BC nonlinear energy fluxes: $Q_{\psi\psi,kl}$, $Q_{\tau\tau,kl}$; Real part of vertical eigenvalues of the linear operator $\hat{L}_p$. The black dashed line is the $-10\% \max_{\mathbf{k}} \left|\langle H_f \rangle_{kl}\right|$ contour of the heat flux field and the black solid curve to corresponding positive one.

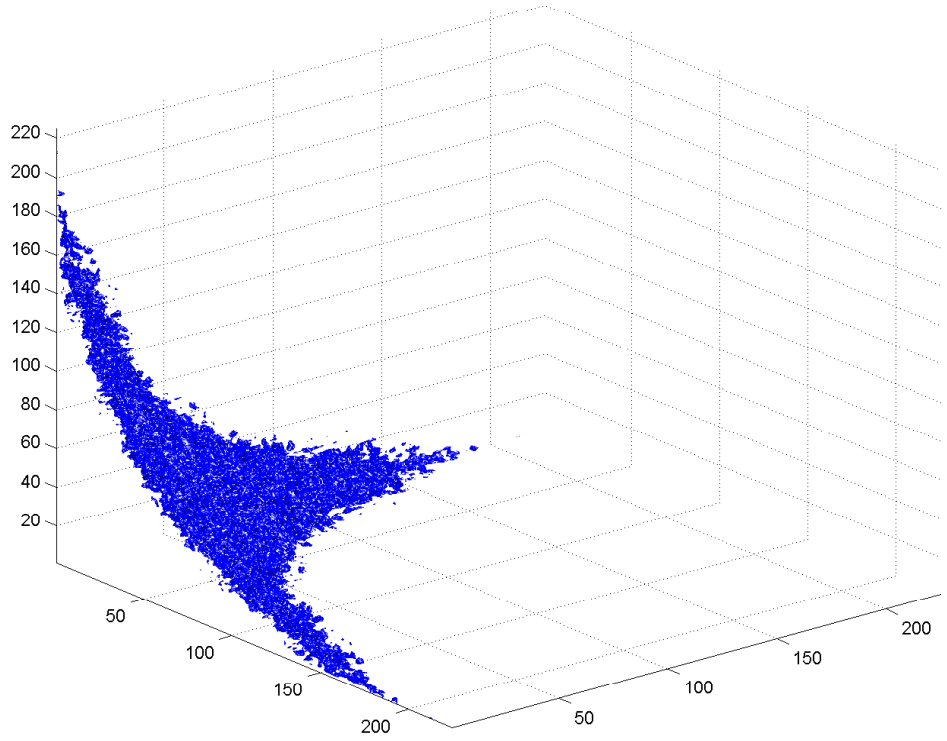

Figure S10: Third order moments having intensity more than 10% of the maximum value. These are shown with respect to EOF modes arranged in descending energy order.